Author Manuscript

Author Manuscript

Author Manuscript

Author Manuscript

HHS Public Access

Author manuscript

Brain Stimul. Author manuscript; available in PMC 2025 June 13.

Published in final edited form as:

Brain Stimul. 2025 ; 18(3): 822–828. doi:10.1016/j.brs.2025.03.006.

Optogenetic stimulation of cell bodies versus axonal terminals generate comparable activity and functional connectivity patterns in the brain

Li-Ming Hsu[a,b,c,*], **Domenic H. Cerri**[a,b,d], **Regina M. Carelli**[e], **Yen-Yu Ian Shih**[a,b,d,**]

[a]Center for Animal MRI, University of North Carolina at Chapel Hill, United States

[b]Biomedical Research Imaging Center, University of North Carolina at Chapel Hill, United States

[c]Department of Radiology, University of North Carolina at Chapel Hill, United States

[d]Department of Neurology, University of North Carolina at Chapel Hill, United States

[e]Department of Psychology and Neuroscience, University of North Carolina at Chapel Hill, United States

Abstract

Optogenetic techniques are often employed to dissect neural pathways with presumed specificity for targeted projections. In this study, we used optogenetic fMRI to investigate the effective landscape of stimulating the cell bodies versus one of its projection terminals. Specifically, we selected a long-range unidirectional projection from the ventral subiculum (vSUB) to the nucleus accumbens shell (NAcSh) and placed two stimulating fibers—one at the vSUB cell bodies and the other at the vSUB terminals in the NAcSh. Contrary to the conventional view that terminal stimulation confines activity to the feedforward stimulated pathway, our findings reveal that terminal stimulation induces brain activity and connectivity patterns remarkably similar to those of vSUB cell body stimulation. This observation suggests that the specificity of optogenetic terminal stimulation may induce antidromic activation, leading to broader network involvement than previously acknowledged.

This is an open access article under the CC BY-NC-ND license (http://creativecommons.org/licenses/by-nc-nd/4.0/).

[*]Corresponding author. Center for Animal MRI, University of North Carolina at Chapel Hill, United States., liming_hsu@med.unc.edu (L.-M. Hsu). [**]Corresponding author. Center for Animal MRI, University of North Carolina at Chapel Hill, United States., shihy@neurology.unc.edu (Y.-Y.I. Shih).

Declaration of competing interest

The authors declare that they have no known competing financial interests or personal relationships that could have appeared to influence the work reported in this paper.

CRediT authorship contribution statement

Li-Ming Hsu: Investigation, Data curation, Software, Resources, and Validation, Writing – review & editing, Writing – original draft, Visualization, Methodology, Formal analysis. **Domenic H. Cerri:** Investigation, Formal analysis and Writing – original draft, Methodology, Data curation. **Regina M. Carelli:** Supervision, Methodology, Validation, Writing – review & editing. **Yen-Yu Ian Shih:** Funding acquisition, Resources, Supervision, and Visualization, Writing – review & editing, Writing – original draft, Project administration, Conceptualization.

Author Manuscript Author Manuscript Author Manuscript Author Manuscript

Keywords

Optogenetics; fMRI; Functional connectivity; Antidromic activation; Ventral subiculum (vSUB); Nucleus accumbens shell (NAcSh)

1. Introduction

Optogenetic stimulation has become a pivotal method for investigating the functional contributions of cell-type and circuit specific activity changes and has been extensively reviewed in the context of its applications in neuroimaging and circuit dissection [1–5]. While it has been documented that terminal optogenetic stimulation can induce antidromic spikes [6,7], it is still generally presumed that stimulating the axonal terminals of a projection would specifically modulate the activity within that pathway and its downstream targets [1,8,9]. Here, we aim to scrutinize this assumption by comparing the optogenetic effects of ventral subiculum (vSUB) cell body versus its projection terminals in the nucleus accumbens shell (NAcSh) through brain-wide fMRI. The vSUB of the hippocampus plays a role in reward and addiction, mediated through its projections to the NAcSh [10–12]. This predominant uni-directional, long-range projection from vSUB to the NAcSh [13] makes it an excellent model for addressing the question proposed herein. Performing optogenetic fMRI on this pathway allows the effects of cell body and terminal stimulations to be unbiasedly compared within subject with minimal invasiveness [6,7,14–21], leaving other irrelevant brain circuits unperturbed and offering brain-wide activity and connectivity patterns that is difficult to access by other recording modalities such as electrophysiology or calcium imaging [22,23].

2. Materials and methods

We used male Sprague-Dawley rats (n = 12, 350–500g, postnatal day 80–120) to conduct optogenetic fMRI experiments targeting the vSUB and its projection terminals in the NAcSh. Rats underwent viral vector injections and optical fiber implantation under anesthesia. They were anesthetized with 2 % isoflurane during surgeries and maintained at 37 °C using a warming pad. Burr holes were drilled above the target areas, and viral vector injections were performed using a microsyringe (30-gauge needle) at 100 nL/min, followed by a 10-min wait for diffusion. Optical fibers (200 μm core, 0.37 NA) were implanted bilaterally and secured with dental cement and screws. Specifically, viral expression was achieved by injecting 1 μl AAV5-CaMKIIα-ChR2-eYFP (ChR2) or control AAV-CaMK2α-eYFP (eYFP) vector (which will not express ChR2) into the vSUB in both hemispheres (AP: 5.75, ML:±4.6, DV: 8.6 mm; from bregma). Bilateral optical fibers were implanted at vSUB (at 0.3 mm above the viral injection target) and NAcSh (AP:+1.3, ML: ±2.2 DV: 6mm; 10° towards midline). This design allowed us to compare activity induced by cell body stimulation versus terminal stimulation within the same animals (Fig. 1A). All animal protocols were approved by the Institutional Animal Care and Use Committee at UNC.

For optogenetic stimulation, a 473 nm laser was used to deliver light pulses through implanted fibers targeting either vSUB cell bodies or their terminals in NAcSh. Stimulation parameters for optogenetic fMRI (ChR2, n = 7; eYFP, n = 6) included 20 Hz frequency,

Author Manuscript Author Manuscript Author Manuscript Author Manuscript

5 ms pulse width, 60-s ON and 120-s OFF blocks repeated five times, with a laser power of 10 mW. For functional connectivity MRI (fcMRI), extended stimulation consisted of a 300-s baseline, followed by alternating ON and OFF periods (300 s each), repeated twice per session. All fMRI experiments were performed under light sedation with 0.5 % isoflurane combined with intravenous dexmedetomidine (0.05 mg/kg/hr) and pancuronium bromide (0.5 mg/kg/hr) [24–27] to maintain stable physiology during imaging. Animals were intubated for mechanical ventilation, and temperature, heart rate, and oxygen saturation were monitored throughout the procedure. A dose of 30 mg/kg monocrystalline iron oxide nanoparticles was used as a contrast agent for cerebral blood volume (CBV) fMRI. fMRI scans were conducted on a 9.4T Bruker scanner equipped with a custom-built surface coil. Single-shot gradient-echo echo-planar imaging (GE-EPI) was used to acquire functional images, with parameters: TR/TE = 1000/8.10 ms, matrix size = 80 × 80, field of view (FOV) = 2.56 × 2.56 cm^2, and slice thickness = 1 mm [25,26]. Prior to functional scans, T2-weighted anatomical images were collected for co-registration and localization of optical fiber placements. Preprocessing of the functional images was carried out using AFNI and custom Python scripts. Images were skull-stripped, slice-time corrected, motion-corrected, smoothness, and co-registered to the anatomical scans [7,28].

Optogenetic fMRI data were analyzed using general linear models (GLM) to estimate stimulus-evoked activity, and voxel-wise activation maps were generated for each subject. For fcMRI, functional connectivity matrices were derived using anatomical regions at the vSUB and NAcSh, and group-level independent component analysis (gICA) (MELODIC; FSL) components calculated from the baseline period. Dual regression was applied to the stimulation period to extract the time series for each gICA component [29].

Lastly, we conducted behavioral tests to assess the motivational and aversive properties of optogenetic stimulation in the vSUB-NAcSh circuit. A separate cohort of adult male Sprague-Dawley rats (n = 12, 350–500 g, postnatal day 80–120) were housed individually under a 12-h light/dark cycle with food and water available ad libitum. Rats were anesthetized with isoflurane (4 % induction, 1.5–2 % maintenance) and placed in a stereotaxic apparatus. Bilateral viral injections of ChR2 (n = 6) or eYFP control vector (n = 6) were performed in the vSUB or NAcSh, as described above. Optical fibers (200 μm core, NA = 0.37) were then implanted 0.3 mm above the injection sites in the NAcSh or vSUB and secured with dental cement and screws. Optogenetic stimulation was delivered through a 473 nm blue laser with parameters of 20 Hz frequency, 5 ms pulse width, and an intensity of 5, 10, or 20 mW, applied continuously for 15 min. Behavioral testing included a self-stimulation task and a stimulation escape task [30,31]. In the self-stimulation task, rats were placed in an operant chamber (Med Associates, Inc.) equipped with a nosepoke sensor, where a nosepoke into the active port triggered a 1-s train of optogenetic stimulation. A 2900 Hz tone (65 dB) was played during the stimulation train, signaling that additional nosepokes during this period would not trigger further stimulation. Nosepokes were recorded as the primary outcome measure. In the stimulation escape task, continuous stimulation was initiated at trial onset for 15 min, with a nosepoke into the active port terminating stimulation for 5 s. A 2900 Hz tone (65 dB) was played immediately after an escape response, marking the stimulation-free period. If no response occurred, stimulation

Author Manuscript Author Manuscript Author Manuscript Author Manuscript

continued uninterrupted. The primary measure in this task was mean stimulation duration, defined as the average time the rat tolerated stimulation before initiating an escape response.

3. Results

Fig. 1 illustrates the brain-wide activity resulting from optogenetic stimulation of vSUB and NAcSh. Bilateral virus expression and optical fiber placement are shown in Fig. 1B–D. Stimulus-evoked fMRI responses were estimated using GLM to fit the stimulation time series. The significant fMRI responses to vSUB and NAcSh stimulation across stimulation frequencies are shown in Fig. 1E and F, while no significant responses were observed in the control group (Fig. 1G). A comparison of the spatial activity patterns between these two stimulation sites revealed overlapping and distinct voxels. Spatial correlation analysis of response maps showed significant spatial correlation between the stimulation conditions, and similar fMRI response (Fig. 1E). To further quantify this similarity, we performed time-to-peak analysis, which revealed no significant differences between the two stimulation conditions across all frequencies (average t-value: 0.474, standard error: 0.53). Additionally, mutual information (MI) analysis demonstrated consistently high MI values (mean: 19.54, standard error: 0.87), further supporting the strong shared information content between the stimulation responses. A random permutation test (1000 iterations) confirmed that these MI values were significantly greater than chance (all p-value <0.000, average t-value: 12.70, standard error: 1.69), reinforcing the robustness of the observed similarity. These data also support the possible existence of antidromic activation, as high frequency stimulations have been reported to more reliably recruit axonal firing. Additionally, full-width at half-maximum (FWHM) (Fig. 1H) and maximum signal CBV response (Fig. 1I) were calculated to evaluate the response shape. A robust spatial correlation was found in FWHM and maximum signal CBV response between vSUB and NAcSh stimulation in the identified overlapping voxel from Fig. 1E.

We also performed resting-state analysis of functional connectivity (FC), summarized in Fig. 2. In the ChR2 group, seed-based analysis of vSUB and NAcSh demonstrated a similar FC pattern during active stimulation (Fig. 2A). Using a one-sample t-test, overlapping voxel distributions were identified, pie charts representing the proportions of voxels in vSUB only, NAc only, or in both vSUB and NAc for the ChR2 group. Correlation analysis indicated a strong spatial correlation in FC patterns between NAcSh and vSUB in the ChR2 group. In contrast, the voxels in eYFP control group showed less overlapping (Fig. 2B). Furthermore, ICA was performed to identify 50 components from the baseline period and then extract time-series to derive the FC matrix from data during stimulation, enabling a data-driven identification of functionally connected networks without prior assumptions (i.e., seed-based FC) (Fig. 2C). We also compared network-level FC changes induced by photo-stimulation (stimulation period – baseline period) and revealed a significantly correlated FC changes between vSUB and NAcSh stimulation, in the ChR2 group, showing a higher network-level similarities than the eYFP control group (Fig. 2D).

To assess whether stimulation site (vSUB vs. NAcSh) influences behavioral outcomes, we analyzed nosepoke responses and mean stimulation duration across three stimulation intensities (5, 10, and 20 mW) using a linear mixed-effects model (LME) with Optogenetic

Author Manuscript Author Manuscript Author Manuscript Author Manuscript

Expression (ChR2 vs. eYFP) and Region (vSUB vs. NAcSh) as fixed factors (Fig. 2E). Across all intensities, there was no significant main effect of Region ($p > 0.05$) and no significant Expression × Region interaction ($p > 0.05$), indicating that stimulation site did not significantly affect self-stimulation or aversive behavior. However, we observed a significant main effect of Expression, with ChR2-expressing rats exhibiting more nosepokes than eYFP controls ($p < 0.05$), demonstrating an intensity-dependent reinforcement effect of vSUB-NAcSh pathway activation. For aversive behavior, only 20 mW stimulation significantly reduced mean stimulation duration in the ChR2 group compared to controls ($p < 0.05$), suggesting an aversive effect at higher intensity, while no significant difference was observed at 10 or 5 mW. These results demonstrate that stimulation site does not differentially impact the behavior examined.

4. Discussion

The results from our study challenge the prevailing assumption that terminal stimulation in optogenetic experiments is highly selective in manipulating the activity within a specific feedforward neural pathway [1,8]. The observed similarity in brain activity and connectivity patterns following vSUB cell body and terminal stimulation in the NAcSh suggests that optogenetic manipulation can induce widespread similar brain-wide effects beyond a single terminal pathway of interest. Our imaging findings offer an empirical overview of terminal stimulation effects. Electrophysiology and calcium-activity measuring techniques in the literature have documented antidromic effects from terminal stimulation, suggesting the possibility to drive the cell bodies and their collaterals, leading to broader network engagement; however, these recording technologies often have a limited scope in capturing the global landscape of brain activity and connectivity [22,23,32–34]. Our work extends beyond this limitation, revealing a more extensive network involvement of terminal stimulations where the recruited circuits can be broader than previously anticipated, mimicking a spatial pattern largely similar to the cell body stimulation.

The implications of these findings underscore the necessity of careful evaluation of the methodological approaches in optogenetic studies, especially when interpreting the specificity and location of neural circuit manipulations. The traditional dichotomy between cell body and terminal stimulation in dissecting neural pathways may be overly simplistic, having insufficient consideration of antidromic signaling from this artificial stimulation of brain circuits [32]. These observations also shed light on the importance of considering the broader neural circuitry and potential feedback mechanisms when designing optogenetic experiments. The antidromic activity and its consequent network-wide connectivity effects reflect the dynamic and interconnected nature of brain circuits, where manipulating one node can reverberate through extensive networks, altering the activity of both directly and indirectly connected regions.

While our study suggests that synaptic terminal stimulation generates activity and connectivity patterns comparable to upstream cell body stimulation, certain limitations warrant further investigation. First, given the inherent temporal resolution constraints of fMRI, we cannot entirely exclude the contribution of indirect network effects. However, since viral injections were restricted to vSUB cell bodies, terminal stimulation at NAcSh is

Author Manuscript Author Manuscript Author Manuscript Author Manuscript

unlikely to recruit circuits irrelevant to the vSUB-NAcSh projection, aside from downstream effects of NAcSh activation, which would also be recruited by vSUB cell body stimulation. This is supported by the highly overlapping voxel-wise responses and strong correlations between two stimulation conditions. If collateral pathways or polysynaptic networks significantly contributed, we would expect greater divergence in activation patterns, time-to-peak variations, and functional connectivity deviations. Nevertheless, future studies integrating electrophysiological approaches with fMRI, such as collision tests [35,36] during whole brain functional mapping, could help further assess the contributions of antidromic activities.

Second, although limited in scope, the behavioral findings reported in this study support the idea that cell body and terminal stimulation can recruit similar motivational and affective responses [10,37,38]. This aligns with our fMRI results, which show substantial overlap in activation patterns between the two conditions and highlight the need for caution when assuming that terminal stimulation alone can selectively manipulate the feedforward pathway and its associated behaviors. While our study advocates for a more cautious interpretation of optogenetic data by integrating findings from both stimulus-evoked fMRI and functional connectivity analyses, this work does not argue that terminal stimulation has no or less specificity compared to cell body stimulation. We believe that terminal stimulation still presents differential stimulation effects compared to direct cell body stimulation, and these effects may still play a pivotal role in modulating behaviors, as reflected in the trending yet statistically insignificant difference observed in our behavioral data. We can, however, conclude that terminal stimulation engages circuits beyond its feedforward pathways and modulates a broader brain-wide activity, including its upstream cell bodies. The brain-wide mapping approach utilized herein can be instrumental in unraveling the complexities of feedforward and feedback neural circuit activities and their respective influences on behavior [39–42]. It is imperative to establish brain-wide imaging techniques suitable for studying network patterns in subjects under behaving conditions [43] to garner a more comprehensive understanding of how specific optogenetic manipulation approaches influence brain function and behavior. This could ultimately aid in developing targeted or closed-loop interventions for neurological and psychiatric disorders. Furthermore, while our study primarily focuses on brain-wide activity and connectivity patterns, future research should investigate how these observed neural effects translate into behavioral outcomes, providing a more comprehensive understanding of the functional implications of optogenetic cell body versus terminal stimulation.

Third, we recognize that our study was conducted in anesthetized animals, which may influence feedback and feedforward circuit dynamics compared to awake, behaving subjects. While the anesthetic protocol used here [7,17,27–29,44–47] has been shown to preserve neurovascular coupling, future work should aim to replicate these findings in awake animals to determine whether similar network-wide effects occur under awake behaving states.

Fourth, a critical consideration in optogenetic fMRI studies is the potential heating effects induced by laser light delivery [48–50]. However, if heating were a major contributor to the observed fMRI responses, we would expect activation to be localized near the fiber tip [48] rather than extending along the targeted circuits and the extended networks. Furthermore,

Author Manuscript Author Manuscript Author Manuscript Author Manuscript

control animals expressing eYFP without ChR2 did not exhibit significant fMRI activity changes, further supporting the specificity of optogenetically driven neural activity. Taken together, these findings suggest that our observed fMRI responses are more likely to reflect neural circuit engagement rather than heating artifacts. Nevertheless, future studies incorporating direct temperature monitoring, such as MR thermometry, would help further validate these observations.

Finally, we did not systematically vary light illumination levels in our fMRI study. However, we acknowledge that adjusting stimulation intensity could influence the balance between antidromic and orthodromic activation, potentially leading to distinct activity and connectivity patterns in the brain. We opted to maintain a fixed light intensity to minimize confounding factors such as heating artifacts, which can induce non-specific fMRI responses unrelated to neuronal activation [48–50]. Additionally, the non-linear relationship between light intensity and opsin activation [51,52], influenced by factors such as desensitization and tissue scattering, could introduce variability that complicates data interpretation. Instead, we prioritized modulation of stimulation frequency, as it more directly influences neuronal firing dynamics and network engagement, providing a clearer framework for investigating functional connectivity.

In conclusion, our investigation into the vSUB versus vSUB-NAc shell optogenetic stimulation using fMRI reveals that the effects of terminal stimulation are not as specific as broadly believed. This insight highlights the need for careful experimental design and interpretation in optogenetic studies. Future research should aim to elucidate the collateral influences underlying the broad network effects or incorporate strategies that avoid recruiting collaterals or employ concurrent silencing of cell body activity to achieve truly specific, pathway-specific terminal stimulation.

Acknowledgments

This study was supported by National Institute of Biomedical Imaging and Bioengineering (R01EB033790), National Institute of Mental Health (R01MH126518, RF1MH117053, S10MH124745), National Institute of Neurological Disorders and Stroke (R01NS128278, R21NS133913), National Institute on Alcohol Abuse and Alcoholism (P60AA011605, U01AA020023), National Institute on Drug Abuse (R21DA057503), National Institute of Child Health and Human Development (P50HD103573), National Institute on Aging (R21AG083589), and NIH Office of the Director (S10OD026796).

References

[1]. Emiliani V, Entcheva E, Hedrich R, Hegemann P, Konrad KR, Lüscher C, et al. Optogenetics for light control of biological systems. Nat Rev Methods Primers 2022;2. 10.1038/s43586-022-00136-4.

[2]. Fenno L, Yizhar O, Deisseroth K. The development and application of optogenetics. Annu Rev Neurosci 2011;34:389–412. 10.1146/annurev-neuro-061010-113817. [PubMed: 21692661]

[3]. Rost BR, Wietek J, Yizhar O, Schmitz D. Optogenetics at the presynapse. Nat Neurosci 2022;25:984–98. 10.1038/s41593-022-01113-6. [PubMed: 35835882]

[4]. Kim CK, Adhikari A, Deisseroth K. Integration of optogenetics with complementary methodologies in systems neuroscience. Nat Rev Neurosci 2017;18:222–35. 10.1038/nrn.2017.15. [PubMed: 28303019]

[5]. Carter ME, de Lecea L. Optogenetic investigation of neural circuits in vivo. Trends Mol Med 2011;17:197–206. 10.1016/j.molmed.2010.12.005. [PubMed: 21353638]

Author Manuscript Author Manuscript Author Manuscript Author Manuscript

[6]. Chen Y, Sobczak F, Pais-Roldán P, Schwarz C, Koretsky AP, Yu X. Mapping the brain-wide network effects by optogenetic activation of the corpus callosum. Cerebr Cortex 2020;30:5885–98. 10.1093/cercor/bhaa164.

[7]. Cerri DH, Albaugh DL, Walton LR, Katz B, Wang T-W, Chao T-HH, et al. Distinct neurochemical influences on fMRI response polarity in the striatum. Nat Commun 2024;15:1916. 10.1038/s41467-024-46088-z. [PubMed: 38429266]

[8]. Deisseroth K Optogenetics: 10 years of microbial opsins in neuroscience. Nat Neurosci 2015;18:1213–25. 10.1038/nn.4091. [PubMed: 26308982]

[9]. McIntyre CC, Savasta M, Kerkerian-Le Goff L, Vitek JL. Uncovering the mechanism (s) of action of deep brain stimulation: activation, inhibition, or both. Clin Neurophysiol 2004;115:1239–48. 10.1016/j.clinph.2003.12.024. [PubMed: 15134690]

[10]. Bossert JM, Adhikary S, St Laurent R, Marchant NJ, Wang H-L, Morales M, et al. Role of projections from ventral subiculum to nucleus accumbens shell in context-induced reinstatement of heroin seeking in rats. Psychopharmacology (Berl) 2016;233:1991–2004. 10.1007/s00213-015-4060-5. [PubMed: 26344108]

[11]. Cooper DC, Klipec WD, Fowler MA, Ozkan ED. A role for the subiculum in the brain motivation/reward circuitry. Behav Brain Res 2006;174:225–31. 10.1016/j.bbr.2006.05.036. [PubMed: 16870273]

[12]. O'Mara S The subiculum: what it does, what it might do, and what neuroanatomy has yet to tell us. J Anat 2005;207:271–82. 10.1111/j.1469-7580.2005.00446.x. [PubMed: 16185252]

[13]. Oh SW, Harris JA, Ng L, Winslow B, Cain N, Mihalas S, et al. A mesoscale connectome of the mouse brain. Nature 2014;508:207–14. 10.1038/nature13186. [PubMed: 24695228]

[14]. Grimm C, Duss SN, Privitera M, Munn BR, Karalis N, Frässle S, et al. Tonic and burst-like locus coeruleus stimulation distinctly shift network activity across the cortical hierarchy. Nat Neurosci 2024;27:2167–77. 10.1038/s41593-024-01755-8. [PubMed: 39284964]

[15]. Kim S, Moon HS, Vo TT, Kim C-H, Im GH, Lee S, et al. Whole-brain mapping of effective connectivity by fMRI with cortex-wide patterned optogenetics. Neuron 2023;111:1732–1747.e6. 10.1016/j.neuron.2023.03.002. [PubMed: 37001524]

[16]. Chen X, Sobczak F, Chen Y, Jiang Y, Qian C, Lu Z, et al. Mapping optogenetically-driven single-vessel fMRI with concurrent neuronal calcium recordings in the rat hippocampus. Nat Commun 2019;10:5239. 10.1038/s41467-019-12850-x. [PubMed: 31748553]

[17]. Menon V, Cerri D, Lee B, Yuan R, Lee S-H, Shih Y-YI. Optogenetic stimulation of anterior insular cortex neurons in male rats reveals causal mechanisms underlying suppression of the default mode network by the salience network. Nat Commun 2023;14:866. 10.1038/s41467-023-36616-8. [PubMed: 36797303]

[18]. Hsu L-M, Shih Y-YI. Neuromodulation in small animal fMRI. J Magn Reson Imag 2024. 10.1002/jmri.29575.

[19]. Wang X, Leong ATL, Tan SZK, Wong EC, Liu Y, Lim L-W, et al. Functional MRI reveals brain-wide actions of thalamically-initiated oscillatory activities on associative memory consolidation. Nat Commun 2023;14:2195. 10.1038/s41467-023-37682-8. [PubMed: 37069169]

[20]. Chuang K-H, Li Z, Huang HH, Khorasani Gerdekoohi S, Athwal D. Hemodynamic transient and functional connectivity follow structural connectivity and cell type over the brain hierarchy. Proc Natl Acad Sci USA 2023;120:e2202435120. 10.1073/pnas.2202435120. [PubMed: 36693103]

[21]. Zou Y, Tong C, Peng W, Qiu Y, Li J, Xia Y, et al. Cell-type-specific optogenetic fMRI on basal forebrain reveals functional network basis of behavioral preference. Neuron 2024;112:1342–1357.e6. 10.1016/j.neuron.2024.01.017. [PubMed: 38359827]

[22]. Grienberger C, Giovannucci A, Zeiger W, Portera-Cailliau C. Two-photon calcium imaging of neuronal activity. Nat Rev Methods Primers 2022;2. 10.1038/s43586-022-00147-1.

[23]. Bakkum DJ, Frey U, Radivojevic M, Russell TL, Müller J, Fiscella M, et al. Tracking axonal action potential propagation on a high-density microelectrode array across hundreds of sites. Nat Commun 2013;4:2181. 10.1038/ncomms3181. [PubMed: 23867868]

[24]. Fukuda M, Vazquez AL, Zong X, Kim S-G. Effects of the α_2-adrenergic receptor agonist dexmedetomidine on neural, vascular and BOLD fMRI responses in the somatosensory cortex. Eur J Neurosci 2013;37:80–95. 10.1111/ejn.12024. [PubMed: 23106361]

Author Manuscript Author Manuscript Author Manuscript Author Manuscript

[25]. Decot HK, Namboodiri VMK, Gao W, McHenry JA, Jennings JH, Lee S-H, et al. Coordination of brain-wide activity dynamics by dopaminergic neurons. Neuropsychopharmacology 2017;42:615–27. 10.1038/npp.2016.151. [PubMed: 27515791]

[26]. Van Den Berge N, Albaugh DL, Salzwedel A, Vanhove C, Van Holen R, Gao W, et al. Functional circuit mapping of striatal output nuclei using simultaneous deep brain stimulation and fMRI. Neuroimage 2017;146:1050–61. 10.1016/j.neuroimage.2016.10.049. [PubMed: 27825979]

[27]. Chao T-HH, Lee B, Hsu L-M, Cerri DH, Zhang W-T, Wang T-WW, et al. Neuronal dynamics of the default mode network and anterior insular cortex: intrinsic properties and modulation by salient stimuli. Sci Adv 2023;9:eade5732. 10.1126/sciadv.ade5732. [PubMed: 36791185]

[28]. Lee S-H, Broadwater MA, Ban W, Wang T-WW, Kim H-J, Dumas JS, et al. An isotropic EPI database and analytical pipelines for rat brain resting-state fMRI. Neuroimage 2021;243:118541. 10.1016/j.neuroimage.2021.118541. [PubMed: 34478824]

[29]. Hsu L-M, Liang X, Gu H, Brynildsen JK, Stark JA, Ash JA, et al. Constituents and functional implications of the rat default mode network. Proc Natl Acad Sci USA 2016;113:E4541–7. 10.1073/pnas.1601485113. [PubMed: 27439860]

[30]. Britt JP, Benaliouad F, McDevitt RA, Stuber GD, Wise RA, Bonci A. Synaptic and behavioral profile of multiple glutamatergic inputs to the nucleus accumbens. Neuron 2012;76:790–803. 10.1016/j.neuron.2012.09.040. [PubMed: 23177963]

[31]. Steiner SS, Beer B, Shaffer MM. Escape from self-produced rates of brain stimulation. Science 1969;163:90–1. [PubMed: 5763497]

[32]. Bukalo O, Campanac E, Hoffman DA, Fields RD. Synaptic plasticity by antidromic firing during hippocampal network oscillations. Proc Natl Acad Sci USA 2013;110:5175–80. 10.1073/pnas.1210735110. [PubMed: 23479613]

[33]. Gover TD, Kao JPY, Weinreich D. Calcium signaling in single peripheral sensory nerve terminals. J Neurosci 2003;23:4793–7. 10.1523/JNEUROSCI.23-12-04793.2003. [PubMed: 12832498]

[34]. Moran A, Stein E, Tischler H, Belelovsky K, Bar-Gad I. Dynamic stereotypic responses of Basal Ganglia neurons to subthalamic nucleus high-frequency stimulation in the parkinsonian primate. Front Syst Neurosci 2011;5:21. 10.3389/fnsys.2011.00021. [PubMed: 21559345]

[35]. Fuller JH, Schlag JD. Determination of antidromic excitation by the collision test: problems of interpretation. Brain Res 1976;112:283–98. 10.1016/0006-8993(76)90284-5. [PubMed: 821582]

[36]. Swadlow HA. Neocortical efferent neurons with very slowly conducting axons: strategies for reliable antidromic identification. J Neurosci Methods 1998;79:131–41. 10.1016/s0165-0270(97)00176-3. [PubMed: 9543479]

[37]. Whishaw IQ, Mittleman G. Hippocampal modulation of nucleus accumbens: behavioral evidence from amphetamine-induced activity profiles. Behav Neural Biol 1991;55:289–306. 10.1016/0163-1047(91)90633-2. [PubMed: 1905533]

[38]. Patterson D, Khan N, Collins EA, Stewart NR, Sassaninejad K, Yeates D, et al. Ventral hippocampus to nucleus accumbens shell circuit regulates approach decisions during motivational conflict. PLoS Biol 2025;23:e3002722. 10.1371/journal.pbio.3002722. [PubMed: 39854559]

[39]. Lindenbach D, Seamans JK, Phillips AG. Activation of the ventral subiculum reinvigorates behavior after failure to achieve a goal: implications for dopaminergic modulation of motivational processes. Behav Brain Res 2019;356:266–70. 10.1016/j.bbr.2018.09.002. [PubMed: 30201390]

[40]. Glangetas C, Fois GR, Jalabert M, Lecca S, Valentinova K, Meye FJ, et al. Ventral subiculum stimulation promotes persistent hyperactivity of dopamine neurons and facilitates behavioral effects of cocaine. Cell Rep 2015;13:2287–96. 10.1016/j.celrep.2015.10.076. [PubMed: 26628379]

[41]. Sesia T, Bulthuis V, Tan S, Lim LW, Vlamings R, Blokland A, et al. Deep brain stimulation of the nucleus accumbens shell increases impulsive behavior and tissue levels of dopamine and serotonin. Exp Neurol 2010;225:302–9. 10.1016/j.expneurol.2010.06.022. [PubMed: 20615406]

Author Manuscript Author Manuscript Author Manuscript Author Manuscript

[42]. Marinescu A-M, Labouesse MA. The nucleus accumbens shell: a neural hub at the interface of homeostatic and hedonic feeding. Front Neurosci 2024;18:1437210. 10.3389/fnins.2024.1437210. [PubMed: 39139500]

[43]. Shih YY, MacKinnon MJ, Ma Y. Methods and systems for functional magnetic resonance imaging with a zero echo time pulse-sequence. US Patent App 2023;17.

[44]. Hsu L-M, Cerri DH, Lee S-H, Shnitko TA, Carelli RM, Shih Y-YI. Intrinsic functional connectivity between the anterior insular and retrosplenial cortex as a moderator and consequence of cocaine self-administration in rats. J Neurosci 2024;44. 10.1523/JNEUROSCI.1452-23.2023.

[45]. Lin T-C, Lo Y-C, Lin H-C, Li S-J, Lin S-H, Wu H-F, et al. MR imaging central thalamic deep brain stimulation restored autistic-like social deficits in the rat. Brain Stimul 2019;12:1410–20. 10.1016/j.brs.2019.07.004. [PubMed: 31324604]

[46]. Grandjean J, Corcoba A, Kahn MC, Upton AL, Deneris ES, Seifritz E, et al. A brain-wide functional map of the serotonergic responses to acute stress and fluoxetine. Nat Commun 2019;10:350. 10.1038/s41467-018-08256-w. [PubMed: 30664643]

[47]. Hsu L-M, Keeley RJ, Liang X, Brynildsen JK, Lu H, Yang Y, et al. Intrinsic insular-frontal networks predict future nicotine dependence severity. J Neurosci 2019;39:5028–37. 10.1523/JNEUROSCI.0140-19.2019. [PubMed: 30992371]

[48]. Schmid F, Wachsmuth L, Albers F, Schwalm M, Stroh A, Faber C. True and apparent optogenetic BOLD fMRI signals. Magn Reson Med 2017;77:126–36. 10.1002/mrm.26095. [PubMed: 26778283]

[49]. Christie IN, Wells JA, Southern P, Marina N, Kasparov S, Gourine AV, et al. fMRI response to blue light delivery in the naïve brain: implications for combined optogenetic fMRI studies. Neuroimage 2013;66:634–41. 10.1016/j.neuroimage.2012.10.074. [PubMed: 23128081]

[50]. Luo H, Yang Z, Yang P-F, Wang F, Reed JL, Gore JC, et al. Detection of laser-associated heating in the brain during simultaneous fMRI and optogenetic stimulation. Magn Reson Med 2023;89:729–37. 10.1002/mrm.29464. [PubMed: 36161670]

[51]. Luboeinski J, Tchumatchenko T. Nonlinear response characteristics of neural networks and single neurons undergoing optogenetic excitation. Netw Neurosci 2020;4:852–70. 10.1162/netn_a_00154. [PubMed: 33615093]

[52]. Mohanty SK, Lakshminarayananan V. Optical techniques in optogenetics. J Mod Opt 2015;62:949–70. 10.1080/09500340.2015.1010620. [PubMed: 26412943]

Author Manuscript Author Manuscript Author Manuscript Author Manuscript

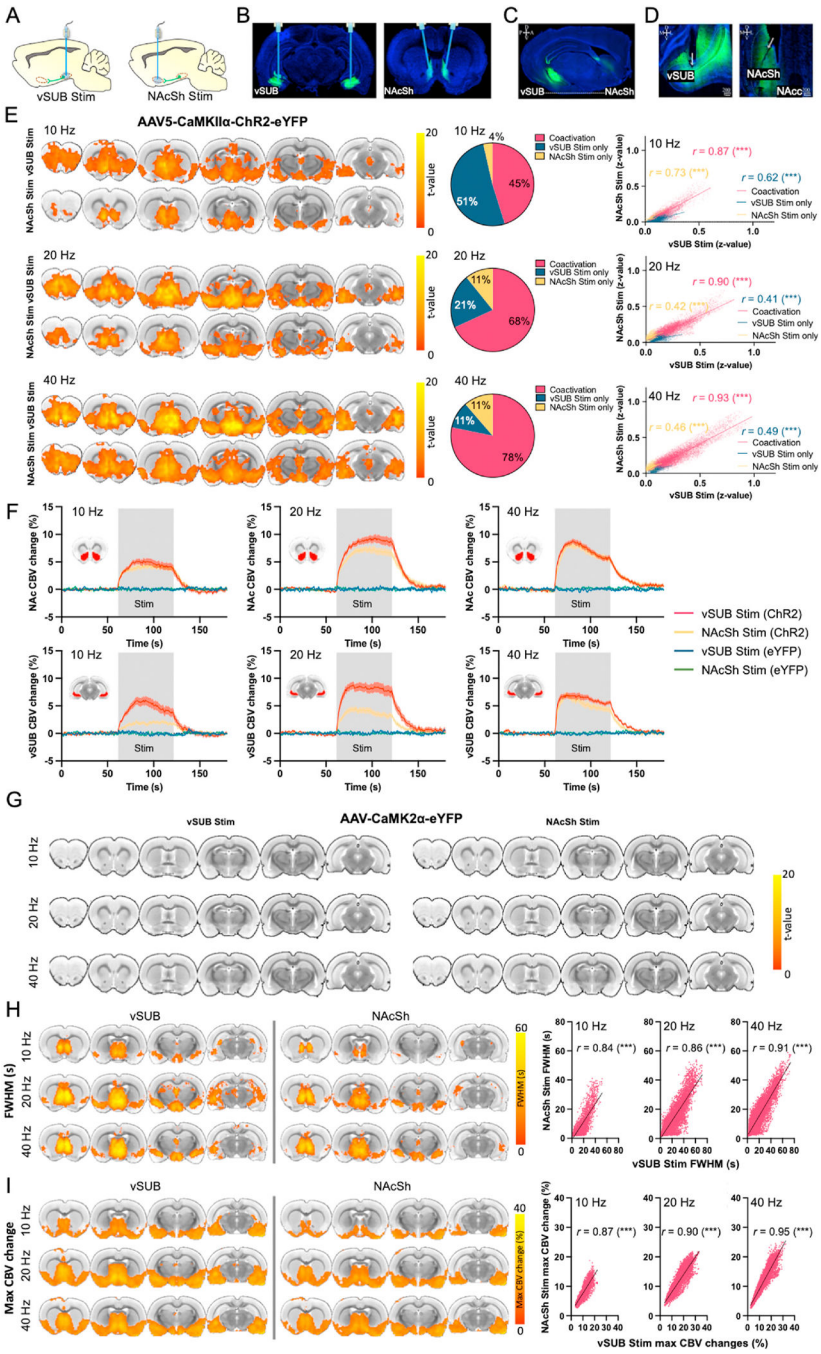

Fig. 1.

Optogenetic stimulation of vSUB cell bodies and their terminals in NAcSh induced similar brain-wide activity patterns. (A) Schematic representation of optogenetic stimulation sites, including the vSUB cell bodies and the NAcSh terminals. (B) Expression of eYFP in vSUB cell bodies and NAcSh terminals (green) against DAPI staining (blue), with corresponding optical fiber placements. (C) Overview of eYFP expression in vSUB-NAcSh terminals. (D) Position of optical fibers (indicated by arrows). (E) Voxel-wise activation maps for both vSUB and NAcSh stimulations across frequencies, showing overlapping voxβel

Author Manuscript Author Manuscript Author Manuscript Author Manuscript

distributions. (one sample *t*-test, corrected $p < 0.05$ using 3dClustSim) Correlation analysis based on the responsive voxels indicated a strong spatial relationship between NAcSh and vSUB stimulation. The voxels were categorized into three groups: voxels in vSUB Stim only, voxels in NAcSh Stim only, and voxels present in both vSUB Stim and NAcSh Stim (coactivation). (F) Average time series derived from the anatomical vSUB and NAc ROIs. (G) One-sample *t*-test of vSUB and NAcSh Stim in eYFP expression group (one sample *t*-test, corrected $p < 0.05$ using 3dClustSim). Analysis of (H) FWHM and (I) maximum CBV changes for each voxel across frequencies, showing a strong relationship between NAcSh and vSUB using the overlapping voxels identified in (E), specifically those present in both vSUB and NAcSh stimulation. (***$p < 0.001$).

Author Manuscript Author Manuscript Author Manuscript Author Manuscript

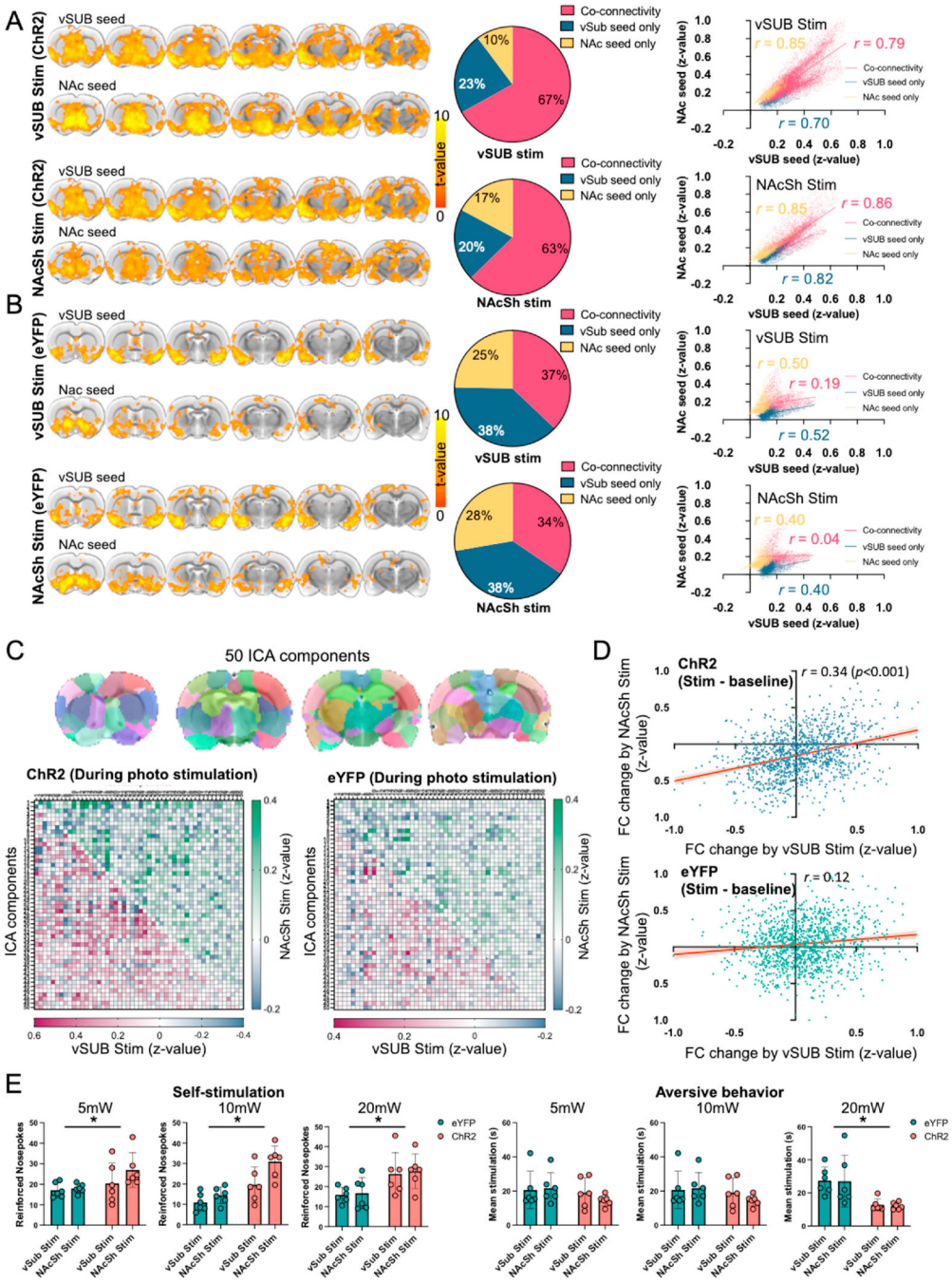

Fig. 2.

Optogenetic stimulation of vSUB cell bodies and their terminals in NAcSh induced similar brain-wide functional connectivity (FC) patterns. (A) Seed-based analysis of vSUB and NAc FC in the ChR2 group showed similar FC patterns with overlapping voxel distributions (one sample *t*-test, corrected $p < 0.05$ using 3dClustSim). Pie chart showing the proportion of voxels categorized as being in vSUB seed only, NAc seed only, or in both vSUB and NAcSh seed (co-connectivity) for the ChR2 group with corresponding correlation analysis between vSUB and NAcSh stimulation for their respective voxels. Correlation analysis based on

Author Manuscript Author Manuscript Author Manuscript Author Manuscript

identified voxels indicated a strong spatial relationship (all p-value <0.001) between NAc and vSUB FC. (B) Identical seed-based FC analysis in the eYFP group does not identify stimulation effects. (C) ICA with 50 components derived from the baseline (pre-stimulation) period, and the FC matrix derived from the vSUB (lower left, purple scale heatmap) and NAcSh (upper right, green scale heatmap) stimulation. (D) Correlation analysis revealed a significantly higher correlation of stimulation-induced FC pattern changes (stimulation - baseline) in the ChR2 group compared to the eYFP group (z-value = 5.72, $p < 0.001$). (E) LME analysis revealed no significant effect of stimulation site (vSUB vs. NAcSh) on behavior, while optogenetic expression significantly increased nosepokes in self-stimulation and decreased mean stimulation in aversive behavior at 20 mW (*$p < 0.05$).